RSC Advances

ROYAL SOCIETY OF CHEMISTRY

www.rsc.org/advances

Journal Name

ARTICLE

Evolution from Small Sized Au Nanoparticles to Hollow Pt/Au Nanostructures with Pt Nanorods and Mechanistic Study

Received 00th January 20xx,
Accepted 00th January 20xx

DOI: 10.1039/x0xx00000x

www.rsc.org/

Ying Ma, Li Xu, Wei Chen, Chao Zou, Yun Yang,* Lijie Zhang,* Shaoming Huang*

A facile method for synthesizing hollow Au/Pt nanostructures is reported and this strategy involves using small sized Au nanoparticles (NPs) as seeds and KI as growth modifier. Under polyvinylpyrrolidone (PVP) and potassium iodide (KI), small sized Au NPs evolved to plate-like nanostructures due to Ostwald ripening. The nanoplates served as templates for selectively growing Pt on {110} facets. Under high temperature, I^- was oxidized to I_2 by O_2. The formed I_2 and KI etched Au on {111}, generating hollow nanostructures. Through adjusting the reaction conditions, dendrite sphere-like nanostructures also could be prepared. The prepared bimetallic Au/Pt nanostructures exhibited high catalytic performance compared with sphere-like Pt.

Introduction

Increasingly serious environmental pollution and rising energy demands have promoted the research of direct methanol fuel cell greatly during the past several decades.[1] Therefore, as the most vital catalyst in fuel cell，platinum (Pt) nanostructures have attracted much attention undoubtedly.[2-20] In comparison with its bulk counterpart, nanostructured Pt materials have high catalytic ability due to size effect. Scientists have found that, besides size, their catalytic abilities also have strong dependence on their shapes. Thus, developing methods to fabricate Pt NPs with various shapes is a very important issue.[21-45] So far, many routes, including seeding growth,[9-15] the introduction of inorganic ion,[16, 17] decomposition of organic Pt precursor under high temperature,[18-29] template-induced growth,[16, 17] galvanic reaction,[35-37] and electrochemical method [38, 39] have been developed to prepare Pt NPs with various shapes including polyhedron,[3] nanowire,[31] nanorod, [6a] branched structure,[18] multipod[23] and dendrite[40-45] successfully. Among them, rod-like nanostructures attract much attention.[46-49] For example, Xia and co-workers fabricated Pt nanorods by using polymeric and ceramic microspheres decorated with Pd NPs as seeds.[46] Liu et al. prepared Pt nanorods supported on carbon nanotubes and investigated their electrocatalytic performance.[47] Lee and co-workers reported the synthesis of five-fold twinned Pt nanorods in alkylamine.[48] Jin and co-workers synthesized Pt nanorods by using mesoporous silica as template.[49] Besides, scientists also paid much attention to hollow Pt-based nanostructures during the last decades because such materials have large specific surface area and excellent catalytic performance.[50-54] Our group synthesized nanocages and nanorings using octahedral and decahedra Au NPs as templates respectively.[50] Hollow Pt-based nanostructures were also synthesized by other groups.[51, 52, 55] For example, Lou et al. synthesized Pt-Cu alloy cubic nanocages through a solvothermal method.[51] Galvanic etching was also used by Shviro et al. for preparing hollow octahedral and cuboctahedral Pt-Ni-Au nanostructures.[52] Considering the advantages of hollow Pt-based nanostructures and nanorods, the synthesis of hollow nanostructures with Pt nanorod is deserved.

Here, we report a facile method which can be used to synthesize hollow Au/Pt nanostructures with high density of Pt nanorods. This strategy involves using water-soluble polymer as reducing agent and protective agent, KI as shape-modifier and growth-induced agent, and 3nm Au NPs as seeds. Mechanstic study demonsted the formation of such nanostructures involved three main steps (The shape transformation of Au seeds from small sized NPs to nanoplates, the selective growth of Pt on {110} of nanoplates, the selective etching on {111} of Au nanoplates). Through adjusting the reaction condition, sphere-like dendrite Pt could be prepared. Electrocatalytic oxidization of methanol was used to investigate their catalytic performance and they exhibited shape-dependent catalytic ability.

Experimental section

Chemicals

Hydrogen tetrachloroaurate(III) hydrate ($HAuCl_4$) and KI were bought from Sigma-Aldrich. Sodium borohydride ($NaBH_4$), chloroplatinic acid (H_2PtCl_6), PVP (Mw=58000) were purchased from Aladdin reagent. All chemicals were not purified before use. Milli-Q Academic water purification system (Millipore Corp., Billerica, MA, USA) was used to prepare deionized water (18.2 MΩ·cm) which was used in all preparations.

Nanomaterials and Chemistry Key Laboratory, Wenzhou University, Wenzhou, Zhejiang, 325027, P. R. China. Email: bachier@163.com; Lizhang@wzu.edu.cn, smhuang@wzu.edu.cn

†Electronic Supplementary Information (ESI) available: [other electrochemical measurements, TEM images, HAADF images, EDS patterns of products prepared under other conditions]. See DOI: 10.1039/x0xx00000x

Synthesis of Au seed NPs

PVP (1 g) was dissolved in water (100 mL) under ultrasonic and then $HAuCl_4$ (0.024M, 1 mL) was added to form a yellow solution. About ice-cold aqueous solution (1 mL) containing $NaBH_4$ (7 mg) was introduced under vigorous magnetic stirring rapidly, causing the color change from yellow to brownish due to the formation of Au NPs. In order to be sure that redundant $NaBH_4$ reacted with water completely, stirring continued for 5 h. Obtained Au colloid needed no any treatment in further preparation of Au/Pt nanostructures.

Preparation of hollow Au/Pt nanostructures

In a standard synthesis, 2 mL above 4 nm Au NPs colloid, 67 uL H_2PtCl_6 aqueous solution (0.019 M), 100 uL water containing 80 mg KI, 50 mg PVP were dissolved in water to form a mixture which was transferred into a 10 mL poly(tetrafluoroethylene) (Teflon)-lined stainless steel autoclave and heated at 180 ^{o}C. After 5h, the heating source was removed and the product was collected by centrifugation (8000 rpm). The obtained precipitates were redissolved in water and subjected to centrifugation again. This treatment was repeated twice and the final products were dispersed in 2 mL water for further characterizations.

Preparation of the cathode

A reported method was used to prepare working cathode with prepared nanostructures. Firstly, a glassy carbon disk electrode with 3.0 mm in diameter was first polished with alumina slurries (0.05 *ί*m) and then subjected to sonication in a water solution containing HNO_3 (0.1 M) , H_2SO_4 (0.1 M) for 10 min successively. Concentrated Pt nanostructures colloid (1.0 mg/mL) was then taken out and dropped on the treated glassy carbon disk electrode surface by a microliter syringe. A gentle heat (40 ^{o}C) was used to dry the catalyst film. In order to remove remaning PVP, the dried film was put in ultraviolet ozone chamber for about 20 min and oxidization could effectively remove organic polymers. After oxidization, ethanol (10 mL) was used to wash the surface of film and purified film was dried again at 40 ^{o}C.

Electrochemical Measurements

Electrochemical measurements were carried out in the electrolyte consisting of H_2SO_4 (0.5 M) and methanol (0.5 M) by using conventional three-electrode cells with a Pt flake of 1 cm^2 area as the counter electrode, an Ag/AgCl-KCl (saturated) electrode as the reference electrode, and the above glassy carbon cathode loaded with active nanocatalysts as the working electrode. All potentials were referenced to Ag/AgCl-KCl (saturated).

The electrochemical performance of the electrodes was investigated by using a PARSTAT 30 Advanced Electrochemical System. The cyclic voltammograms (CV) of methanol oxidation were measured at the scan rate of 20 mV/s in the potential range of 0 V to 1.0 V at room temperature. The chronoamperometry curves were obtained by polarizing the electrode at 0.65 V for 2000 s in the above-mentioned electrolyte. Before each test, the solution was purged with N_2 for 30 min to eliminate the dissolved oxygen.

Characterizations

5 uL above purified colloid was deposited on copper grids coated by thin carbon film and dried at 80 ^{o}C. After water was removed completely, samples were observed with a 300 KV Tecnai G2 F30 S-T-Twin microscope attached with high angel annular dark field detector (HAADF) and X-ray energy dispersive spectrometer (EDS).

Result and discussion

The structure of Au/Pt nanostructures

Fig. 1 shows the representative HAADF and TEM images of as-synthesized bimetallic Au/Pt nanostructures, clearly implying that most of products are hollow. However, the products shapes are not monodispersed (70% are frame-like and others are hollow sphere) (Fig. 1A). In most cases, the caves are very small so that the hollow structure was hardly observed. When the size of cave is large enough, the HAADF and TEM images can offer a clear hollow image (Fig. 1B and 1C). HRTEM images show that the products are composed of short nanorods. EDS analysis demonstrated these short nanorods were Pt (Fig. 1E). From Fig. 1 D, the interval between adjacent lattice fringes was 0.23nm, close to the lattice spacing of {111} of fcc Pt. This demonstrates that the short rod grew along <111> direction.

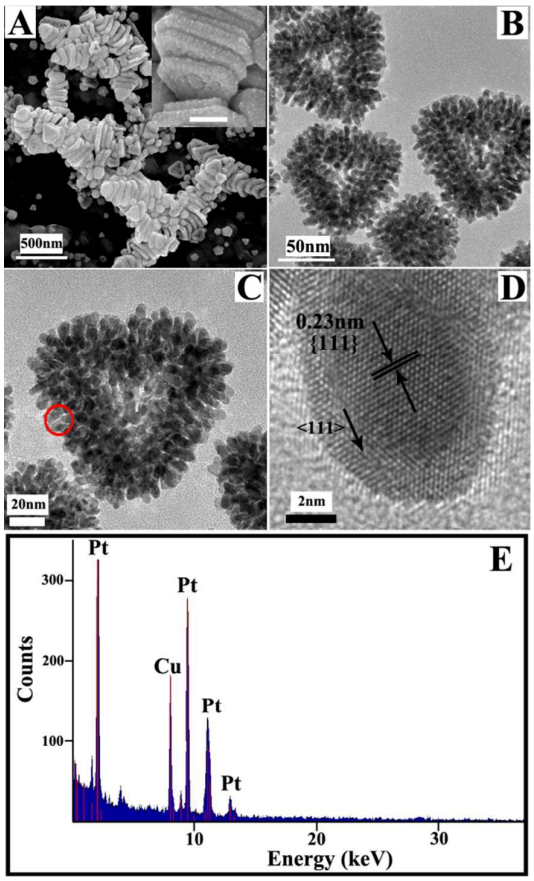

Fig 1. (A-D) SEM and TEM images of hollow nanostructures prepared using a standard synthesis (inset in Fig. 1 A is the SEM image at high magnification and scale bar is 100 nm). (E) EDS pattern of area marked by red circle in C.

The structure with reaction time and possible mechanism

In order to investigate the formation mechanism, the intermediate products with different growth times were taken out and observed with SEM and TEM (Fig. 2). Before reaction, the Au seeds (Fig. 2A) were monodispersed and had 4 nm mean size. HRTEM image (Fig. 2A) indicates that these used Au NPs were well single crystalline. After the system was heated for 10 min, fine NPs disappeared and products became polydispersed (Fig. 2B). Nanoplates including triangle and pentagon with large size were observed. Meanwhile, qusi-shpere NPs also formed (Fig. 2B1). HRTEM image shows that the lattice distance is 0.24 nm and matches the {111} of Au (Fig. 2B2). EDS was further applied to identify their composition and result showed that they were Au (Fig. 2B3). Note that the surface of plate NPs was smooth at this stage. Upon reacting time prolonging to 1h, the surface of plate-like nanostructures became rough and protuberance-like structures were observed clearly on their surfaces (Fig. 2C). STEM-EDS and EDS analyses gave a detailed elemental distribution (Fig. C3 and Fig. S1). Au was the main composition and small amount of Pt was observed, indicating that the smoothing was due to the growth of Pt. Clearly, above result shows that pt preferentially grew on {110} facets and no significant growth occurred on {111} facet. When the reaction time was prolonged to 5 h, hollow nanostructures formed (Fig. 1 and 2D). Fig. 2D2 is the STEM-EDS analysis of one NP. Distinctively, Au was not removed completely and therefore products had Au@Pt structure precisely. The remained Au from Au nanoplate was coated by deposited Pt atoms. Based on the EDS analysis, the molar ratio of Au and Pt in final product is 0.11 (Fig. S3).

Though the evolving mechanism of the NP is not understood fully so far, a possible mechanism involving three key steps might be adopted to explain this. **(I) The formation of nanoplate was resulted from Ostwald ripening and the absorption of KI on {111}** (Scheme 1). Previously, Lee's group demonstrated shape evolution from spherical Ag NPs to other shapes (plate and rod).[54] They believed that Ostwald ripening and selective-absorption of PVP on specific crystal facet were responsible for the shape evolution. In our system, the formation of plate possibly followed their mechanism partly. Initially, under the PVP and high temperature, small-sized Au NPs reconstructed to nanoplates. However, it must be noted that KI also is a key factor to the formation of nanoplate. When preparation occurred without KI, obtained products were significantly different and no plate-like nanostructures formed (Fig. 3A and 3B). Only small sized NPs formed. This demonstrated that KI also strongly affected the formation of nanoplate. It can be understood theortically. Well known, I^- ions has strong complexing interaction with Au atoms.[56-58] Thay is why I^- is involved in the synthesis of Au nanostructures, especially Au nanoplate.[58] In our system, it is believed that I^- absorbed on {111} facet of nanostructures and faciliated the formation of nanoplates. When the amount of KI and PVP were changed, the product shape with different shapes formed, also indicating that KI and PVP affected the formation of nanoplate and in turn the resulting strutcutures of products (Fig. S4-S7).

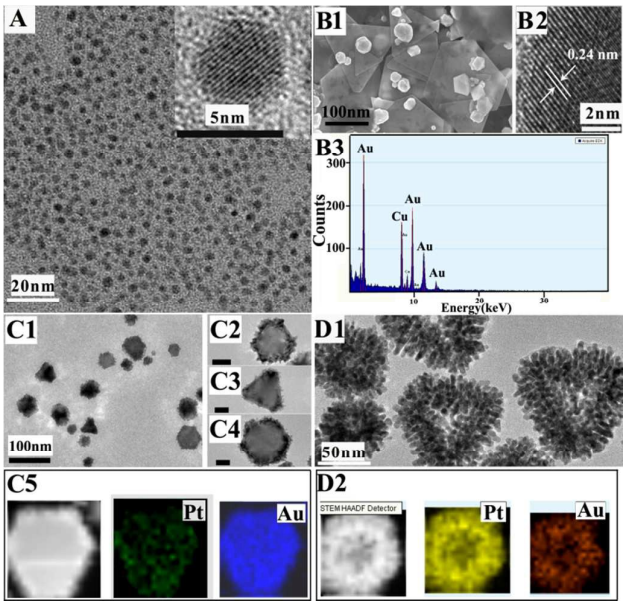

Fig 2. The TEM images, SEM images, EDS pattern and STEM-EDS profiles of products prepared using a standard synthesis which has procceeded for different times: (A) 0h (inset is the HRTEM of one NP); (B1-B3) 10 min; (C1-C3) 1h (The scale bars in Fig. 2C2-C3 are 20 nm); (D1-D2) 5h.

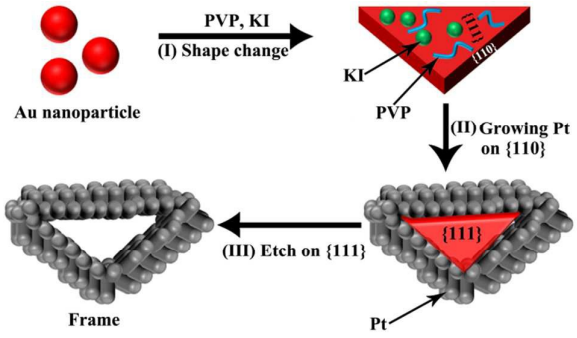

Scheme 1. Schematic illustration of nanoframe

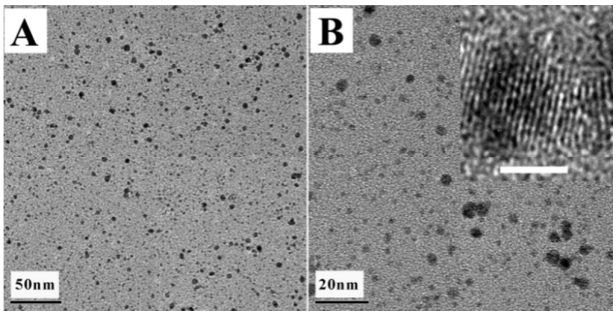

Fig 3. TEM images of products prepared using a standard procedure except that no KI was introducted. Inset is the HRTEM image of one NP (scale bar is 2 nm).

(II) The growth of Pt on {110} (Scheme 1). Further reaction caused the reducation of Pt ions to Pt atoms which deposited on Au nanoplates. Due to the selective absorption of KI and PVP on {111}, the atoms here were not active.[56-58] As a result, the growth of Pt mainly occurred on {110}. Therotically, {110} has

higher free energy than {111} and this also faciliates the growth on {110} instead of {111}. Previously, we demonstrated that the etching could generate active sites which induced selective growth.[50] However, in this system, no significant etching was observed before this stage. Therefore, two proceeses might be different because reaction conditions are not identical. For example, before the growth of Pt, the first stage mainly involved Ostwald ripening. However, no such ripening was invloved in previous preparation.[50] Besides, the templates here mainly were large sized nanoplates and however decahedra acted as templates in previous report.[50] TEM images show that the growth on {110} was highly selective even without etching. This is possibly due to the free energy difference between {110} and {111}. In our previous report,[50] the selective etching along [100] was indispensable to the growth on {100}. However, the selective growth on {110} of nanoplate needed no etching. Well known, {111}, {100} and {110} are commonly observed low index facets on nanostructure surface. Energitically, the order is {110}>{100}>{111}. When decahedra seeds were used as templates, in order to achieve selective growth on {100}, etching was needed to increase free energy difference between {100} and {111}. However, when nanoplates served as templates herein, etching was not necessary because the free energy difference between {111} and {110} was large enough to achieve selective growth on {110}.

(III) The etching on {111} and formation of nanoframe (Scheme 1). Previously, we have demonstrated that KI could be oxidizated to I_2 slowly in high temperature, which could be accelerated by acid.[50, 58] As is well know, the solution containing KI and I_2 have strong ability to etch gold, which is widely used in gold industry.[53] In our system, H_2PtCl_4, used as Pt precursor, could offer an acidic environment, possibly promoting the oxidization of I^- to I_2. Besides, the high temperature (180 ^oC) also could accelerate the reaction. The formed I_2 selectively etched {111} facets together with KI, resulting in formation of caves (Scheme 1). Generally, the etching prefers starting from facet with high surface free energy. For three commonly observed crystal facets, the atoms on {110} is more vulnerable to etching than these on other facets, which is not in agreement with our result. In our system, the growth of Pt on {110} is respobsible for this disagreement. Compared with Au, Pt is a stable metal and can resist the etching of KI/I_2. When Pt atoms grew on {110} and they protected the atoms here against etching.[50] Consequently, the etching preferred occurring on {111} and generated nanoframe.

It is worthnoting that some quasi-shpere NPs were also formed possibly due to Ostwald ripening. This demonstrates that the ripening did not occurred homogenously. So far it is difficult to exactly give a mechanism for the interactions between noble metals and other substances are very complex, for example I^- and Au.[56-58] To figure out a more reasonable mechanism, more experiments are still underway in our laboratory.

The effect of Au seeds

During the formation of nanoframes, Au seeds also played important roles. We caried out the preparation without Au seeds. In this case, TEM and SEM images show that no any frame-like nanostructures formed and only monodipsersed sphere-like Pt dendrite nanostructures with mean 85 nm diameter were observed (Fig. 4). This was a typical growth of NPs. Initially Pt clusters formed and acted as seeds on which subsequent formed Pt atoms deposited and created dendrite sphere (Fig. 4). Clearly, this result suggests that the present Au seeds were important to the formation of nanoplates and subsequental nanoframes. However, when Au seeds were present, they transformed to Au nanoplates which served as seeds for Pt deposition.

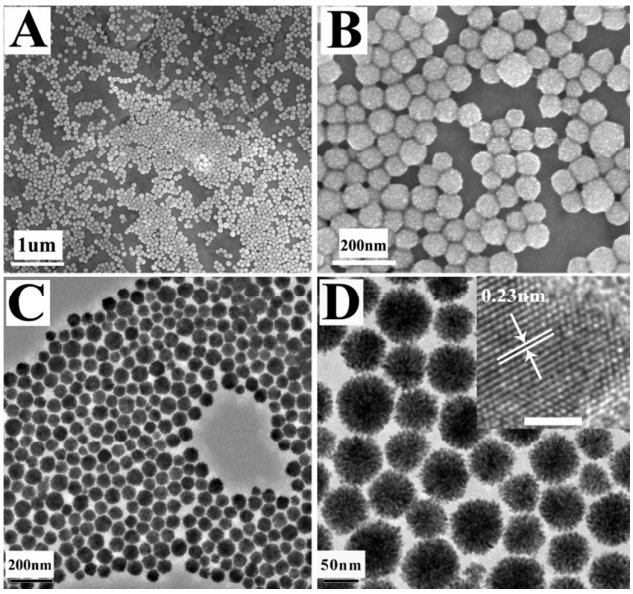

Fig 4. (A-D) SEM and TEM images of monodispersed Pt NPs prepared using a standard synthesis except for that no Au seeds were added. Inset in Fig. 4 D is the HRTEM image of product (Scale bar is 2 nm).

The shape-dependent catalytic performance

Pt-based nanostructures were widely investigated in the electrocatalytic oxidization of methanol.[47, 60-63] Previously, several groups had demonstrated Pt nanorods were excellent catalysts because there were exposed high-index facets on their surfaces.[60, 63] The hollow Au/Pt nanostructures prepared using our method are composed of Pt short nanorods with high density. Therefore, they might be potential catalyst in the electrocatalytic oxidization of methanol and we carried out the electrocatalytic test of Au/Pt nanostructures shown in Fig. 1. Besides, the catalytic performance of dendrite sphere shown in Fig. 4 was also investigated. Fig. 5A shows that both catalysts gave the typical methanol oxidation current peak on Pt catalyst. The peak position in the positive direction was at about 0.70 V and 0.45 V in the reverse direction.[60] Significantly, their peak current densities were different. In the positive scanning, the hollow Au/Pt nanostructures had a peak current density (500 mA/mg) (Curve 1 in Fig. 5A). The current denisty of dendrite Pt sphere was 100 mA/mg in the same scanning direction (Curve 2 in Fig. 5A). We have demonstrated that commerical Pt/C had a 60 mA/mg peak current density

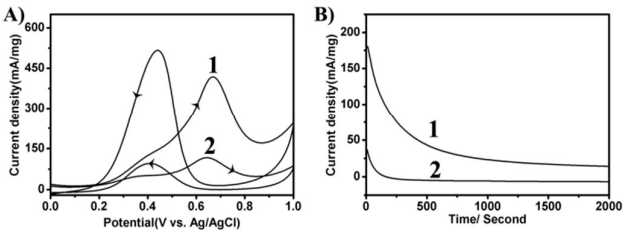

Fig. 5. The properties of electrocatalytic oxidation of methanol using nanostructures (Curve 1 and Curve 2 were recorded using hollow Au/Pt nanostructures shown in Fig. 1 and dendrite Pt nanostructures shown in Fig. 4 respectively): (A) Cyclic voltammograms at a scan rate of 20 mV/s; (B) Corresponding current-time curves measured at 0.3 V. All measurements were carried out in a mixture of 0.1M methanol and 0.5M H_2SO_4 at 25 ^{o}C. The arrows in Fig. 5 A indicate the scanning direction. For hollow Au/Pt nanostructures, their mass activity of the final products was normalized by the total mass of Au and Pt.

previously.[63] It can be known that both Au/Pt nanostructure and dendrite Pt sphere exhibited higher catalytic performance than commerical Pt/C. Among them, hollow Au/Pt nanostructures have the highest calatytic ability. Besides, the stability of hollow Au/Pt nanostructures also were advantageous over dendrite Pt nanospheres (**Fig. 5B**) possibly due to the synergistic effect between Pt and Au which increased resistance to CO.[61]

Conclusion

We have demonstrated a wet-chemical method involving using 4 nm Au NPs as seeds, PVP as protective agents and reducing agent, KI as shape-modifier, H_2PtCl_6 as Pt precursor for syntheizing hollow Au/Pt nanostructures with dense Pt nanorods on their surface. KI is a critical factor which faciliates the transformation of Au seed from sphere to nanoplate. Besides, KI could be partly oxidizated to I_2 which acted as etchant for creating hollow Au/Pt nanostructures. Through adjusting reaction condition, dendrite Pt nanospheres could also be prepared. These prepared nanostructures exhibit shape- and composition-dependent catalytic performance. This method possibly provides a simple route to rebuild materials structures and shapes. The prepared materials are potential catalysts in fuel cell.

Acknowledgements

This work was supported by the NSFC (21471117, 21173159, 21173159, 61471270 and 51420105002).

Notes and references

1 L. Carrette, K. A. Friedrich and U. Stimming, *Fuel Cells*, 2001, **1**, 5.
2 Z. Peng and H. Yang, *Nano Today*, 2009, **4**, 143.
3 J. Chen, B. Lim, E. P. Lee and Y. Xia, *Nano Today*, 2009, **4**, 81.
4 A. R. Tao, S. Habas and P. Yang, *Small*, 2008, **4**, 310.
5 A. Chen, P. Hot-hindle, *Chem. Rev.*, 2010, **116**, 3767.
6 M. Subhramannia and V. K. Pillai, J. *Mater. Chem*., 2008, **18**, 5858.
7 X. Wang, J. Zhuang, Q. Peng and Y. Li, *Nature*, 2005, **437**, 121.
8 W. Chen, J. Kim, L. Xu, S. Sun and S. Chen, *J. Phys. Chem. C*, 2007, **111**, 13452.
9 K. Niesz, M. Grass and G. A. Somorjai, *Nano Lett.*, 2005, **5**, 2238.
10 W. He, X. Wu, J. Liu, K. Zhang, W. Chu, L. Feng, X. Hu, W. Zhou and S Xie, *Langmuir* 2010, **26**, 4443.
11 F. Fan, D. Liu, Y. Wu, S. Duan, Z. Xie, Z. Jiang and Z. Tian, *J. Am. Chem. Soc*., 2008, **130**, 6949.
12 F. Liu, J. E. Hu, Q. Wang, K. Gaskell, A. I. Frenkel, G. I. Jackson and B. Eichhorn, *J. Am. Chem. Soc.*, 2009, **131**, 6924.
13 B. Lim, M. Jiang, P. H. C. Camargo, E. C. Cho, J. Tao, X. Lu, Y. Zhu and Y. Xia, *Science*, 2009, **324**, 1302.
14 H. Lee, S. E. Habas, G. A. Somorjai and P. Yang, *J. Am. Chem. Soc*., 2008, **130**, 5406.
15 L. Feng, X. Wu, L. Ren, Y. Xiang, W. He, K. Zhang, W. Zhou and S. Xie, *Chem. Eur. J*., 2008, **14**, 9764.
16 J. Chen,T. Herricks and Y. Xia, *Angew. Chem. Int. Ed*., 2005, **44**, 2589.
17 M. E. Grass, Y. Yue, S. E. Habas, R. M. Rioux, C. I. Teall, P. Yang and G. A. Somorjai, *J. Phys. Chem. C*, 2008, **112**, 4797.
18 Z. Fang, Y. Zhang, F. Du and X. Zhong, *Nano Res*., 2008, **1**, 249.
19 Z. Peng and H. Yang, *J. Am. Chem. Soc.*, 2009, **131**, 7542.
20 S. Cheong, J. Watt, B. Ingham, M. F. Toney and R. D. Tilley, *J. Am. Chem. Soc*., 2009, **131**, 14590.
21 S. L. Lim, I. Ojea-Jiménez, M. Varon, E. Casals, J. Arbiol and V. Puntes, *Nano Lett.*, 2010, **10**, 964.
22 J. Zhang and J. Fang, *J. Am. Chem. Soc.*, 2009, **131**, 18543.
23 X. Teng and H. Yang, *Nano Lett.*, 2005, **5**, 885.
24 H. Zhang, J. Ding and G. M. Chow, *Langmuir*, 2008, **24**, 375.
25 C. Wang, Y. Hou, J. Kim and S. Sun, *Angew. Chem. Int. Ed.*, 2009, **46**, 6333.
26 C. Wang, H. Daimon and S. Sun, *Nano Lett.*, 2009, 9, 1493. (i) J. Ren and R. D. Tilley, *Small*, 2007, *3*, 1508.
27 J. D. Hoefelmeyer, K. Niesz, G. A. Somorjai and R. D. Tilley, *Nano Lett.*, 2005, **5**, 435.
28 S. M. Humphrey, M. E. Grass, S. E. Habas, K. Niesz, G. A. Somorjai and T. D. Tilley, *Nano Lett*., 2007, **7**, 785.
29 S. Choi, R. Choi, S. Han and J. Park, *Chem. Commun.*, 2010, **46**, 4950.
30 F. Liu, J. Lee and W. Zhou, *Adv. Funct. Mater*., 2008, **15**, 1549.
31 A. K. Prashar, R. P. Hodgkins, J. N. Chandran, P. R. Rajamohanan and R. N. Devi, *Chem. Mater*., 2010, **22**, 1633.
32 Q. Yuan, Z. Zhou, J. Zhuang and X. Wang, *Chem. Mater.*, 2010, **22**, 2395.
33 Q. Yuan, Z. Zhou, J. Zhuang and X. Wang, *Chem. Commun.*, 2009, 6613.
34 S. Kundu and H. Liang, *Langmuir*, 2010, **26**, 6720.
35 X. Huang, H. Zhang, C. Guo, Z. Zhou and N. Zheng, *Angew. Chem*.**.,** 2009**, 121,** 4902.
36 M. Mohl, A. Kumar, A. L. M. Reddy, A. Kukovecz, Z. Konya, I. Kiricsi, R. Vajtai and P. M. Ajayan, *J. Phys. Chem. C,* 2010*,* **114**, 389.
37 S. Guo, Y. Fang, S. Dong and E. Wang, *J. Phys. Chem. C*, 2007, **111**, 17104.
38 N. Tian, Z. Zhou, S. Sun, Y. Ding and Z. Wang, Z. *Science*, 2007, **316**, 732.
39 Z. Zhou, Z. Huang, D. Chen, Q. Wang, N. Tian and S. Sun, *Angew. Chem. Int. Ed.*, 2010, **49**, 411.
40 Y. Song, Y. Yang, C. J. Medforth, E. Pereira, A. K. Singh, H. Xu, Y. B. Jiang, C. J. Brinker, C. J. Swol and F. Shelnutt, *J. Am. Chem. Soc*., 2004, **126**, 635.
41 M. Sanles-Sobrido, M. A. Correa-Duarte, S. Carregal-Romero, B. Rodríguez-González, R. A. Álvarez-Puebla, P. Hervés and L. M. Liz-Marzán, *Chem. Mater*., 2009, **21**, 1531.

42 L. Wang, H. Wang, Y. Nemoto and Y. Yamauchi, *Chem. Mater*., 2010, **22**, 2835.
43 Y. Li and Y. Huang, *Adv. Mater*., 2010, **22**, 1921.
44 M. A. Mahmoud, C. E. Tabor, M. El-Sayed, Y. Ding and Z. Wang, *J. Am. Chem. Soc*., 2008, **130**, 4590.
45 S. Song, R. Liu, Y. Zhang, J. Feng, D. Liu, Y. Xing, F. Zhao and H. Zhang, *Chem. Eur. J*., 2010, **12**, 6251.
46 E. P. Lee, Z. Peng, D. M. Cate, H. Yang, C. T. Campbell and Y. Xia, *J. Am. Chem. Soc*., 2007, 129, 10634.
47 C. Zhou, X. Du, H. Liu, S. P. Ringer and Z. Liu, *RSC Adv.*, 2015, 5, 80176.
48 J. Yoon, N. T. Khi, H. Kim, B. Kim, H. Baik, S. Back, S. Lee, S.-W. Lee, S. J. Kwon and K. Lee, *Chem. Commun*. 2013, **49**, 573.
49 L. Yang, X. Song, M. Qi, L. Xia and M. Jin, *J. Mater. Chem*., 2013, **1**, 7316.
50 N. N. Fan, Y. Yang, W. F. Wang, L. J. Zhang, W. Chen, C. Zou and S. M. Huang, *ACS Nano,* 2012, **6**, 4072.
51 B. Y. Xia, H. B. Wu, X. Wang and X. W. Lou, *J. Am. Chem. Soc*., 2012, **134**, 13934.
52 M. Shviro, S. Polani and D. Zitoun, *Nanoscale*, 2015, **7**, 13521.
53 F. Saleem, B. Xu, B. Ni, H. Liu, F. Nosheen, H. Li and X. Wang, *Adv. Mater*., 2015, **27**, 2013.
54 T. C. Deivaraj, L. L. Neeta and J. Y. Lee, *Journal of Colloid and Interface Science*, 2005, **289**, 402.
55 H.-J. Jang, S. Ham, J. A. I. Acapulco Jr., Y. Song, S. Hong, K. L. Shuford and S. Park, *J. Am. Chem. Soc*., 2014, **136**, 17674.
56 D. K. Smith, N. R. Miller and B. A. Korgel, *Langmuir,* 2009, **25**, 9518.
57 S. Hong, Y. Choi and S. Park, *Chem. Mater*., 2011, **23**, 5375.
58 L. S. Silbert and D. Swern, *Anal. Chem*., 1958, **30**, 385.
59 P. A. Lyday, "*Iodine and Iodine Compounds" in Ullmann's Encyclopedia of Industrial Chemistry*, 2005, Wiley-VCH, Weinheim.
60 J. Yoon, H. Baik, S. Lee, S. J. Kwon and K. Lee, *Nanoscale*, 2014, **6**, 6434.
61 K. Eid, H. Wang, V. Malgras, Z. A. Alothman, Y. Yamauchi and L. Wang, *J. Phys. Chem. C*, 2015, **119**, 19947.3
62 C. Z. Zhu, D. Du, A. Eychmüller and Y. Lin, *Chem. Rev.*, 2015, **115**, 8896.
63 X. Z. Gong, Y. Yang and S. M. Huang, *Chem. Commun*., 2011, **47**, 1009.

